Talanta 179 (2018) 9–14

Contents lists available at ScienceDirect

Talanta

journal homepage: www.elsevier.com/locate/talanta

A paper-based SERS test strip for quantitative detection of Mucin-1 in whole blood

Shan-Wen Hu, Shu Qiao, Jian-Bin Pan, Bin Kang*, Jing-Juan Xu*, Hong-Yuan Chen

State Key Laboratory of Analytical Chemistry for Life Science and Collaborative Innovation Center of Chemistry for Life Sciences, School of Chemistry and Chemical Engineering, Nanjing University, Nanjing 210023, China

ARTICLE INFO

Keywords:
Paper-based test strip
SERS
Whole blood
Mucin-1
Au NPs

ABSTRACT

A paper-based SERS test strip combining strengths of paper chip and Raman active substrate was demonstrated to overcome challenges in spectroscopic sensing of complicated samples and realize quantitative detection of disease markers in whole blood. The precisely controlled Au NPs were not only capable of generating condensed hot spots on the fibers, but also enhanced the size exclusion effect of paper, resulting in the novel performance on both SERS detection and sample pretreatment. A biosensor for Mucin-1 is developed by equipping the Au NPs with aptamer. Combining all these merits, this small, cheap and portable test strip might find wide application in clinical diagnosis and health evaluation.

1. Introduction

Point-of-care testing (POCT) has experienced booming development over the past decade, offering advantages such as miniaturization, automation and on site. They benefit public health in worldwide especially in developing countries, and show significant potential in clinical diagnosis and health evaluation [1,2].

Surface-enhanced Raman spectroscopy (SERS) could be a promising POCT technique since it can provide fingerprint information of target molecules with high sensitivity. There are two mechanisms attributed to SERS effect, namely, chemical enhancement based on the charge transfer between substrate and analytes, and electromagnetic field (EF) enhancement, which relies on the metallic nanoparticles (NPs) [3,4]. For EF-based SERS detection, nanoparticle synthesis and assembly is the key subject. Some carefully designed nanomaterials have exhibited novel SERS performance [5,6], but simple and low-cost methods of fabricating SERS substrates are in great demand. Though many efforts have been made, there are still some problems unaddressed. Firstly, uniformity is still undesirable since random aggregation of nanoparticles usually generate hot spots with inhomogeneous distribution. Secondly, detachment of nanoparticles leads to poorly reproducible Raman signals. Thirdly, most of the substrates lack the capability of complicated samples such as blood and urine [7–10]. Therefore, a practically applicable SERS-based sensor requires an efficient SERS active substrate that features sensitivity, uniformity and stability [11].

Paper-based chips open new door to executing SERS detection on POCT devices for its promising specialties resulted from the novel physical and chemical properties of paper [2,12,13]. They are cheap in price and relatively easy for shaping, patterning and reagent immobilization. Their porous and fibrous structure makes them an ideal hydrophilic channel for liquid transport with certain size exclusion effect without external pumps [14,15]. Plasmonic nanoparticles could be integrated with paper fibers via multiple ways, such as seeded growth [16], self-assemble [17], adsorption [10], brushing [18], inkjet printing [19] or in situ synthesis [8,20]. The relative standard deviation (RSD) of paper-based SERS substrate could be well controlled down to ~15%. [10]. Thus far, though SERS detection of serum [21], tear [22] and other biological samples [23,24] have been realized on paper, performing SERS detection in whole blood sample still remains challenging. Centrifugation is usually required to remove interference from large number of blood cells [13]. Utilizing direct blood cell separation on paper, SERS detection of glucose in whole blood sample has been explored [25]. Compared with blood glucose that is usually at ~mM level in blood, the concentration of some specific disease marker might be down to nM, which is much more difficult to quantify in whole blood.

Herein, we constructed a uniform paper-based SERS test strip via in situ synthesis of Au NPs on paper fibers. The Au NPs homogeneously stick to paper fibers were not only capable of generating condensed hot spots on the fibers, but also enhanced the size exclusion effect of paper. By equipping Au NPs with aptamer, this SERS test strip was enabled to quantitatively detect Mucin-1, a cancer marker, in whole blood samples. Combining with portative spectrometers, this SERS strip might be as potential test strip for the point-of-care analysis.

* Corresponding authors.
E-mail addresses: binkang@nju.edu.cn (B. Kang), xujj@nju.edu.cn (J.-J. Xu).

http://dx.doi.org/10.1016/j.talanta.2017.10.038
Received 5 September 2017; Received in revised form 16 October 2017; Accepted 20 October 2017

2. Experiment

2.1. Materials, equipment and apparatus

Chlorauric Acid (HAuCl4), $KHCO_3$, citric acid, and glucose were analytically pure from Sigma and used as received without further purification. Phosphate buffered saline (PBS) was purchased from Keygen Biotech Ltd. Doubly deionized water (DI water, 18.2 MΩ at 25 °C) prepared by a Milli-Q (MQ) water system was used throughout all experiments. The DNA oligonucleotide probes used in this study were purchased from Shanghai Sangon Biotechnology Co., Ltd. (Shanghai, China). The thiol-modified Mucin-1 aptamer had the following sequences:

5′-HS-AAAAAGCAGTTGATCCTTTGGATACCCTGGT-3′.

While the complementary sequence was

5′-AAAGGAAAGGATCAACTGCTTTTA-CY5-3′.

The Mucin-1 peptide with two repeats of the 20 amino acid variable tandem repeat region (from the N terminus to the C terminus: PDTRP APGST APPAH GVTSA PDTRP APGST APPAH GVTSA) was purchased from Chinapeptides Biotechnology Co., Ltd. (Shanghai, China). Whatman quantitative filter paper (slow) was purchased from GE Healthcare Life Sciences (Tokyo, Japan).

Scanning electron microscope (SEM, JEOL S-4800) was used for paper morphology characterization. The X-ray photoelectron spectroscopy (XPS) spectrum was recorded by ESCALB MK-II, (VG Co., England) (under a base pressure of 1×10^{-9} Torr using monochromatic Mg-K_α X-rays at $h_\nu = 1253.6$ eV). Raman spectra were recorded by Laser confocal Raman Microspectrometry (inVia-Reflex, Renishaw, England)

2.2. Fabrication of AuNPs on paper

The reaction kittle (50 mL) was filled with 20 mL doubly deionized water containing 3 g citric acid together with 1.875 mL ethanediamine, and heated to 150 °C for 5 h with paper substrate. After thoroughly washed with DI water, the paper was subject to AuNPs deposition. Plating solution contained 12 mM $HAuCl_4.4H_2O$, 4 M $KHCO_3$ (heated to 60 °C for dissolution) and 30 mM glucose was mixed and sat quietly at room temperature for an hour before the carbon dots modified paper was put in. Chemical plating was proceeded at 30 °C with continuously mild shaking (65 r/min).

2.3. SERS detection on strip

Standard 4-MBA solutions with different concentrations were dropped on paper and incubated for 1 h. The paper was washed 3 times by water before SERS detection. The SERS signal on paper is measured using 633 nm laser, every data point was the average of 16 spectra.

DNA solutions were prepared in 25 mM Tris buffer (pH = 7.4) containing 100 mM NaCl unless otherwise stated. The strip was dropped with 20 μL 0.5 μM aptamer and incubated for 8 h before wash, 20 μL 0.5 μM mercaptoethanol was applied to the paper for 1 h. Then the paper was thoroughly washed (5 times) with PBS, applied to 20 μL 2.0 μM Cy5-labeled DNA for 3 h before wash. Then the Paper strip was allowed to dry out before further analysis.

The previously prepared paper strip was applied with different concentrations of Mucin-1 solutions for 1 h and washed out. The Raman signal on paper was measured as mentioned above.

Blood of human with heparin was added to as prepared paper strip, incubated for 1 h before wash, the Raman signal on paper was measured as mentioned above.

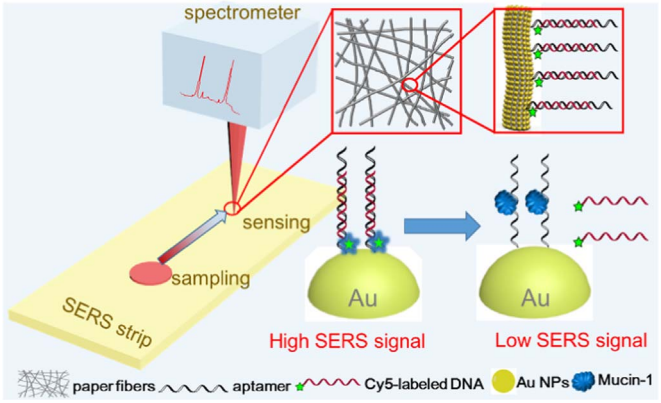

Scheme 1. Concept and design of the paper-based SERS test strip.

3. Results and discussion

3.1. Au NPs decorated on paper

This paper strip is designed as Scheme 1. Au NPs are decorated on paper fibers via a carbon dots assistant strategy, making the strip capable of both sampling and sensing. SEM images in Fig. 1a4 and Fig. S1 show the fibers remain quasi-three-dimensional structure after covered by Au NPs. Raman signal from reporter molecules can be efficiently enhanced by Au NPs within close distance, which lays the foundation of biosensing.

Au NPs are synthesized on this paper strip through a carbon dots assistant strategy (see Supporting Information for details). Carbon dots synthesized on paper by hydro thermal reaction play an essential role during the following Au NPs deposition. SEM images (Fig. 1a2) show that the morphology of paper after hydro thermal reactions is obviously different from bare paper. The X-ray photoelectron spectroscopy (XPS) characterization (Fig. S3) demonstrates the generation of carbon dots [26,27]. After the Au NPs deposition, we can find that fibers in different sizes are all well covered with condensed Au NPs from SEM images in Fig. S1. Since the hot spots of SERS detection rely on Au NPs distribution, this paper strip is capable of controlling the distribution of hot spots. By this means, we have modified the paper with Au NPs without disturbing the original structure of paper fiber. Carbon dots modified paper fibers can accelerate the reduction of $AuCl_4^-$, leading to different reaction rate with solution beyond fibers, which makes the $AuCl_4^-$ tends to be reduced within the fiber and eventually results in the novel distribution of the Au NPs [28–31]. As comparison, we deposit Au NPs on bare paper without carbon dots modification (named as Au-bare-Paper). Clear difference is witnessed between Fig. S1a and Fig. S1b, proving the effect of carbon dots. The in situ synthesized Au NPs are bonded tightly to the paper substrate, hence we can wash the strip thoroughly without worrying about the detachment of nanoparticles during the detection process.

This paper strip exhibits novel performance on sample pretreatment. Since the hydrophilic fibers are covered by Au NPs, the hydrophilicity of strip is changed. Droplets infiltrate into bare paper within less than 1 s, suggesting the hydrophilicity is excellent. When it comes to the strip, contact angle of droplets is larger, and droplets infiltrate the paper slowly in 3 min, indicating the hydrophilicity decreases, which is in favor of Raman sensing [32].

Different from economically developed world, it is difficult to have access to medical tools, trained personnel and diagnostic devices in developing countries. However, it is still challenging for POCT devices used in blood samples due to the complicated environment and affluent blood cells. Most proposed POCT devices require purified blood plasma for analysis. When human blood samples are dropped on the as prepared paper strip, it is capable of triggering blood coagulation since

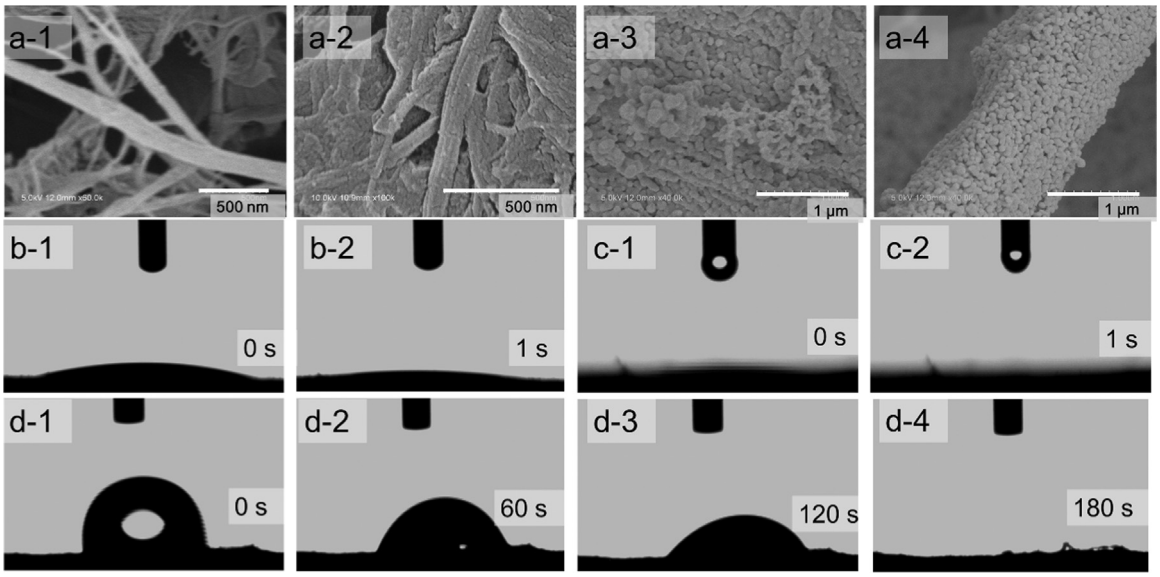

Fig. 1. The morphology and hydrophilicity control of paper-based SERS strip. (A) SEM images of (a1) bare paper, (a2) carbon dots modified paper, (a3) Au NPs deposited on bare paper, (a4) Au NPs deposited on carbonized paper; (B) Photograph of droplets on different substrate showing the hydrophilicity change of strip. (b1-b2) bare paper at initial and 1 s, (c1-c2) carbonized paper at initial and 1 s, (d1-d4) Au NPs modified paper at initial, 60 s, 120 s and 180 s.

condensed Au NPs enhanced the size exclusion effect of filter paper [27,33]. Obvious blood cell coagulation is found on Au NPs modified paper (in Fig. S2 a3), which is different from bare paper or carbon dots modified paper. We also have checked the paper surface 2 mm away from the dropping spot, blood cells or residual are found on bare paper or carbon dots modified paper, while no residual is found on paper strip. This paper strip demonstrates the capability of automatic plasma extraction.

3.2. SERS performance of the strip

Condensed Au NPs make this strip an ideal SERS substrate. 4-Mercaptobenzoic acid (4-MBA) is chosen as Raman reporter because it has strong characteristic Raman peaks at 1412 cm^{-1} (carboxyl stretching vibration), 845 cm^{-1} (carboxyl bending vibration), 1588 cm^{-1} (C-C stretching vibration) and 1078 cm^{-1} (stretching vibration of substituent group on benzene ring). Peak at 1078 cm^{-1} is used for SERS detection. As mentioned before, the carbonized fiber can accelerate the nucleation stage, which results in the unique distribution of Au NPs. This helps to improve the uniformity in two aspects. For one thing, as shown in Fig. S3, fibers at different sizes are fully covered by Au NPs, eliminate the otherness. Furthermore, we can find many clusters on Au-bare-Paper (Fig. S4), which will result in random distribution of hot spots. While on paper strip (Fig. 2c) Au NPs tend to stick to fibers tightly, leading to Raman hot spots in high density and good uniformity.

To demonstrate the uniformity of SERS signal on this strip, we record the 2D mapping data of Raman signal after applying Raman reporter 4-MBA on paper. The uniformity of signal on paper strip is much better than that on Au-bare-Paper. An area is chosen on a paper fiber and mapping image of 4-MBA signal is shown in Fig. 2b, the relative standard deviation (RSD) is calculated to be less than 8% in an 8 μm × 12 μm range, while on Au-bare-Paper it is 51%. We further compare the Raman spectra on different fibers. We choose five fibers with different size and record Raman spectra of seven different spots on each fiber. The average spectra of every fiber are shown in Fig. 2d, the colors on line represent the intensity of signal while the pink shadow represent the RSD. The RSD of peak area at 1078 cm^{-1} is less than 7%, demonstrating a high uniformity within and between fibers. We choose 4-MBA as a model target to demonstrate the potential of quantitative analysis. Peak area at 1078 cm^{-1} increases when the concentration of 4-MBA increases from 5 nM to 100 μM, as shown in Fig. S5, which lays the foundation for direct quantitative analysis on this paper based strip.

3.3. Quantitative detection of Mucin-1 on the strip

Herein, we choose Mucin-1, a transmembrane protein which is identified as a cancer biomarker for breast, ovarian, prostate, and pancreatic, as a model disease target for clinical diagnosis [34,35]. Principle of this aptamer based biosensing process for Mucin-1 is shown in Scheme 1. Briefly the Au NPs on paper strip are equipped with aptamer of Mucin-1 via Au-S with thiol labeled at the 5′ terminus. Then the aptamer is hybridized with a complementary DNA (reporter DNA) labeled by CY-5 at the 3′ terminus [36–38]. When the target is identified by the aptamer, the complementary DNA will be replaced from the aptamer and can be washed away, which leads to the decrease of SERS signal.

Characteristic peaks at 1360, 1230, and 1120 cm^{-1} correspond to the methine chain deformation, C-N stretching vibration, ring-breathing of the CY-5 molecule, respectively [39]. These characteristic peaks can be distinguished from Raman spectrum recorded on paper (Fig. 3a), showing the reporter DNA is captured by the aptamer immobilized on Au NPs and the Raman signal of CY-5 can be efficiently enhanced by Au NPs. The Au NPs are stable enough for thorough rinsing, which is beneficial for this working principle. The ratio between aptamer and the complementary DNA is optimized to avoid un-hybridized aptamer on Au NPs. In Fig. S6 we can find the aptamer is adequately hybridized when the ratio between complementary DNA and aptamer is increased to 4:1. In order to get the highest initial signal, the concentration of aptamer is also optimized. The peak area reaches maximum when the concentration of aptamer is 2.0 μM.

To demonstrate the sensitivity of the strategy, different concentrations of Mucin-1 are added to the paper strip and the Raman signals are measured (Fig. 3b), while the corresponding 2D mapping data of Raman signal is shown in Fig. S7. As expected, a gradual decrease in the SERS intensity of peak at 1360 cm^{-1} is observed as the concentrations of Mucin-1 ranged from 50 ng/mL to 50 μg/mL, indicating the remaining reporter DNA has a log linear correlation with Mucin-1 concentrations. The correlation equation is Y = 60897-10217*X (R^2 = 0.984), where Y is the peak area and X is the log of Mucin-1 concentrations.

To evaluate the selectivity of this approach, other common proteins

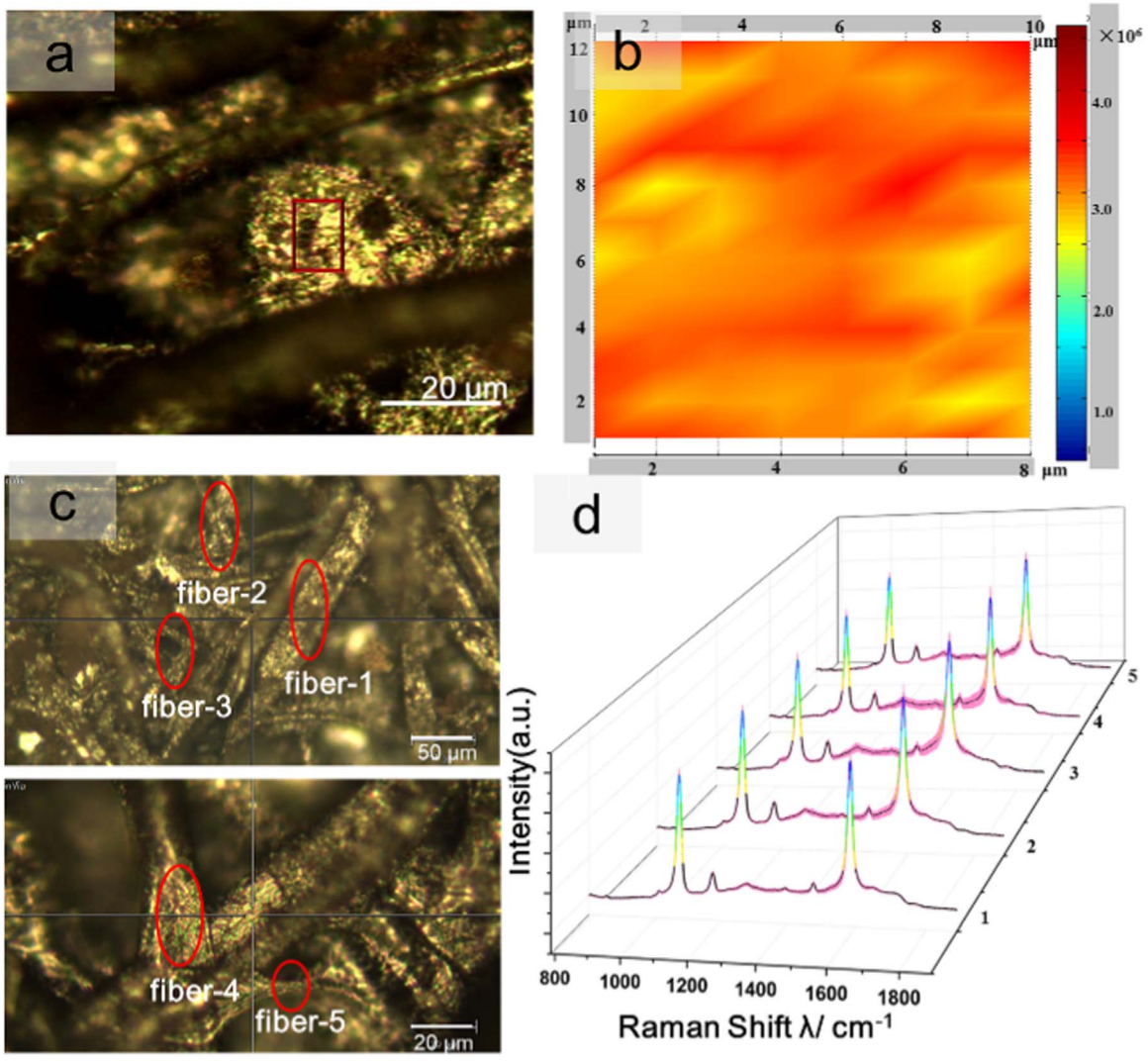

Fig. 2. SERS performance of this strip with 4-MBA. (a) Micrograph of paper strip showing the sensing area. (b) 2D mapping image of 4-MBA (1.0 μM) SERS signal on fiber marked by red square in (a). (c) Micrograph of paper strip showing the sensing spots. (d) Averaged spectra were shown as colored line and their standard deviation was highlighted as pink color, each averaged spectra are 7 spectra chosen on fiber marked by red circles in (c). (For interpretation of the references to color in this figure legend, the reader is referred to the web version of this article.)

including CEA, PSA and BSA at the same concentration of 1.0 μg/mL are added to the paper strip. No significant signal loss compared with the initial intensity are witnessed while Mucin-1 at same concentration can efficiently decrease the SERS signal. An artificial serum sample consisting of common substances such as BSA, globin, triglyceride and salts is also added to the paper strip, the results confirm the ability of this paper strip to tolerate complex sensing environment. These results shown in Fig. 3d indicate that this approach possess a high selectivity toward the target Mucin-1.

Then we perform the Mucin-1 detecting assay with human blood samples. The SERS signal of paper is recorded after thorough rinsing. The concentrations of Mucin-1 in human blood samples are determined based on the working curve in Fig. 3c. A recovery assay is executed to prove the reliability of this test (shown in Fig. 3e). Recovery ratios between 90% and 110% are obtained, which indicate the possible interference from the sensing environment is negligible. Five human blood samples obtained from healthy adults are determined, the results are shown in Fig. 3f. The detected concentrations are consistent with reported Mucin-1 level in normal adults [37]. These results demonstrate the proposed paper strip to be a feasible and promising platform for SERS-based quantitative detection in clinical applications.

4. Conclusions

In conclusion, a paper-based SERS test strip for quantitative detection of Mucin-1 in whole blood is proposed. On this SERS active substrate, in situ synthesized Au NPs stick to paper fibers in high density, which results in condensed Raman hot spots. Inspired by the high uniformity, we develop a quantitative SERS detection of Mucin-1 on this paper-based substrate. Furthermore, this strip exhibits good performance on human blood samples. Considering the versatility of Au NPs as SERS substrates for biosensing, this paper strip could be applicable for the quantitative detection of a wide variety of targets.

Acknowledgement

This work was supported by the National Natural Science Foundation of China (21327902, 21535003, 21675081), State Key Laboratory of Analytical Chemistry for Life Science (5431ZZXM1611), Fundamental Research Funds for the Central Universities (020514380101), and Priority Academic Program Development of Jiangsu Higher Education Institutions.

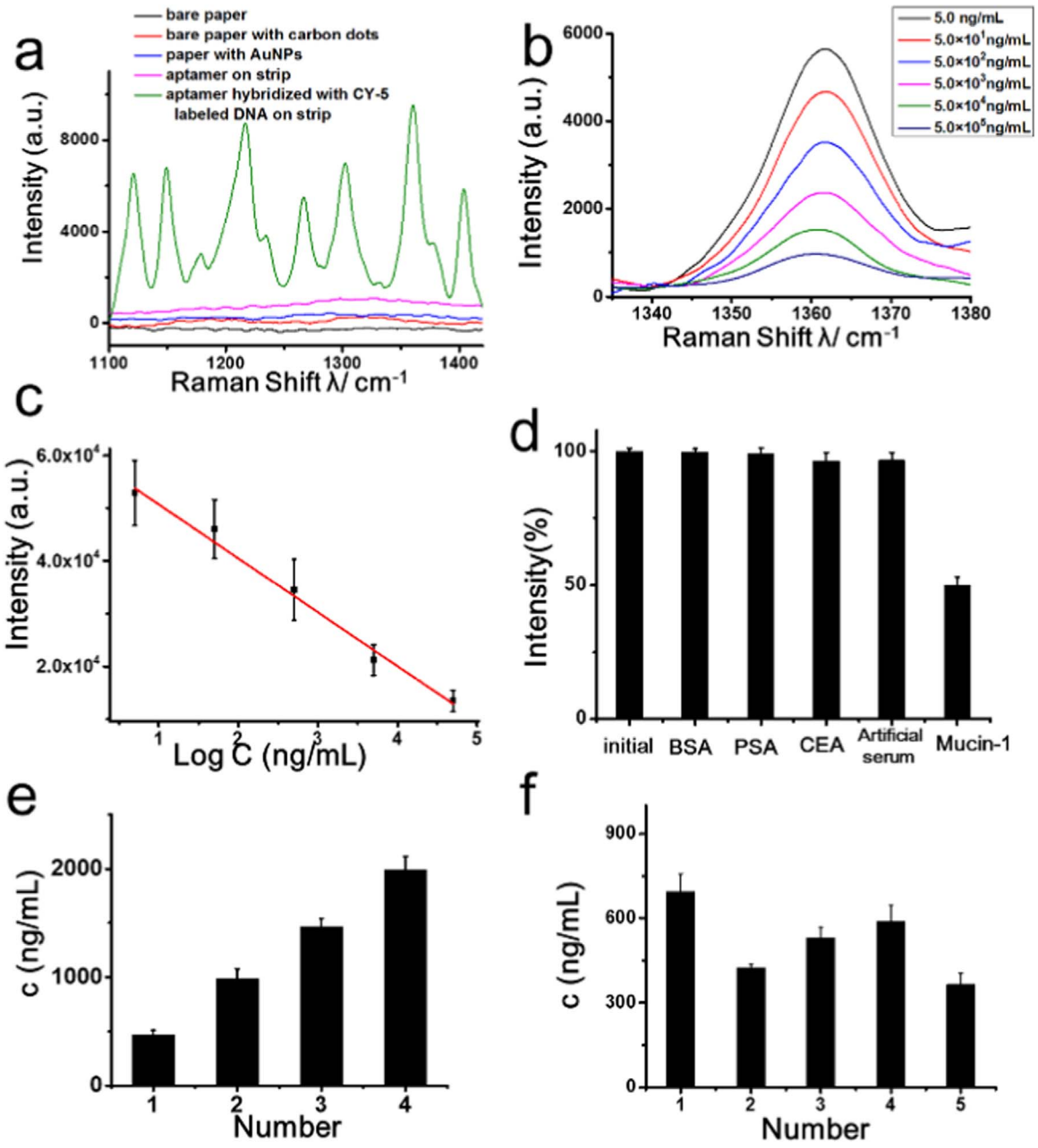

Fig. 3. Quantitative detection of Mucin-1 in human blood samples. (a) Raman spectra of paper, paper with carbon dots, paper strip, paper strip with aptamer modification, paper strip with aptamer and CY-5 labeled reporter DNA. (b) Raman spectra showing peaks at 1360 cm^{-1} with different Mucin-1 concentrations. (c) The linear fitting curve of peak area changing with Mucin-1 concentrations. (d) Specificity test of this Strip with some common proteins and artificial serum. (e) Results of the recovery test on Strip with human blood. The sample number from 1 to 4 refer to blood added 0, 500, 1000 and 1500 ng/mL Mucin-1. (f) Mucin-1 detection results for 5 human blood samples.

Appendix A. Supplementary material

Supplementary data associated with this article can be found in the online version at http://dx.doi.org/10.1016/j.talanta.2017.10.038.

References

[1] D.M. Cate, J.A. Adkins, J. Mettakoonpitak, C.S. Henry, Recent developments in paper-based microfluidic devices, Anal. Chem. 87 (2015) 19–41.
[2] J. Hu, S.Q. Wang, L. Wang, F. Li, B. Pingguan-Murphy, T.J. Lu, F. Xu, Advances in paper-based point-of-care diagnostics, Biosens. Bioelectron. 54 (2014) 585–597.
[3] W. Shen, X. Lin, C.Y. Jiang, C.Y. Li, H.X. Lin, J.T. Huang, S. Wang, G.K. Liu, X.M. Yan, Q.L. Zhong, B. Ren, Reliable quantitative SERS analysis facilitated by core-shell nanoparticles with embedded internal standards, Angew. Chem. Int. Ed. 54 (2015) 7308–7312.
[4] R.R. Frontiera, A.I. Henry, N.L. Gruenke, R.P. Van Duyne, Surface-enhanced femtosecond stimulated raman spectroscopy, J. Phys. Chem. Lett. 2 (2011) 1199–1203.
[5] S.S. Chen, X.X. Lin, A.J. Wang, H. Huang, J.J. Feng, Facile synthesis of multi-branched AgPt alloyed nanoflowers and their excellent applications in surface enhanced Raman scattering, Sens. Actuators B 248 (2017) 214–222.
[6] J.J. Feng, L. Liu, H. Huang, A.J. Wang, Poly(ionic liquid)-assisted one-pot synthesis of Au hyperbranched architectures for enhanced SERS performances, Sens. Actuators B 238 (2017) 91–97.
[7] N. Chen, P. Ding, Y. Shi, T.Y. Jin, Y.Y. Su, H.Y. Wang, Y. He, Portable and reliable surface-enhanced raman scattering silicon chip for signal-on detection of trace trinitrotoluene explosive in real systems, Anal. Chem. 89 (2017) 5072–5078.
[8] G.C. Zheng, L. Polavarapu, L.M. Liz-Marzan, I. Pastoriza-Santos, J. Perez-Juste, Gold nanoparticle-loaded filter paper: a recyclable dip-catalyst for real-time reaction monitoring by surface enhanced Raman scattering, Chem. Commun. 51 (2015) 4572–4575.
[9] A. Saha, N.R. Jana, Paper-based microfluidic approach for surface-enhanced raman spectroscopy and highly reproducible detection of proteins beyond picomolar concentration, ACS Appl. Mater. Interfaces 7 (2015) 996–1003.
[10] C.H. Lee, M.E. Hankus, L. Tian, P.M. Pellegrino, S. Singamaneni, Highly sensitive surface enhanced raman scattering substrates based on filter paper loaded with plasmonic nanostructures, Anal. Chem. 83 (2011) 8953–8958.

[11] T.Y. Jeon, D.J. Kim, S.-G. Park, S.-H. Kim, D.-H. Kim, Nanostructured plasmonic substrates for use as SERS sensors, Nano Converg. 3 (2016) 18.
[12] J.F. Betz, W.W. Yu, Y. Cheng, I.M. White, G.W. Rubloff, Simple SERS substrates: powerful, portable, and full of potential, Phys. Chem. Chem. Phys. 16 (2014) 2224–2239.
[13] X. Gao, P. Zheng, S. Kasani, S. Wu, F. Yang, S. Lewis, S. Nayeem, E. Englerchiurazzi, J. Wigginton, J.W. Simpkins, A paper-based surface-enhanced raman scattering lateral flow strip for detection of neuron-specific enolase in blood plasma, Anal. Chem. 89 (2017) 10104–10110.
[14] A.W. Martinez, S.T. Phillips, M.J. Butte, G.M. Whitesides, Patterned paper as a platform for inexpensive, low-volume, portable bioassays, Angew. Chem. Int. Ed. 46 (2007) 1318–1320.
[15] C.M. Cheng, A.W. Martinez, J.L. Gong, C.R. Mace, S.T. Phillips, E. Carrilho, K.A. Mirica, G.M. Whitesides, Paper-based ELISA, Angew. Chem. Int. Ed. 49 (2010) 4771–4774.
[16] Z.J. Gong, H.J. Du, F.S. Cheng, C. Wang, C.C. Wang, M.K. Fan, Fabrication of SERS swab for direct detection of trace explosives in fingerprints, ACS Appl. Mater. Interfaces 6 (2014) 21931–21937.
[17] S.K. Sivaraman, V. Santhanam, Realization of thermally durable close-packed 2D gold nanoparticle arrays using self-assembly and plasma etching, Nanotechnology 23 (2012) 255603.
[18] W. Zhang, B.W. Li, L.X. Chen, Y.Q. Wang, D.X. Gao, X.H. Ma, A.G. Wu, Brushing, a simple way to fabricate SERS active paper substrates, Anal. Methods 6 (2014) 2066–2071.
[19] P. Joshi, V. Santhanam, Paper-based SERS active substrates on demand, RSC Adv. 6 (2016) 68545–68552.
[20] W. Kim, Y.H. Kim, H.K. Park, S. Choi, Facile fabrication of a silver nanoparticle immersed, surface-enhanced raman scattering imposed paper platform through successive ionic layer absorption and reaction for on-site bioassays, ACS Appl. Mater. Interfaces 7 (2015) 27910–27917.
[21] A.G. Berger, S.M. Restaino, I.M. White, Vertical-flow paper SERS system for therapeutic drug monitoring of flucytosine in serum, Anal. Chim. Acta 949 (2017) 59–66.
[22] M. Park, H. Jung, Y. Jeong, K.-H. Jeong, Plasmonic schirmer strip for human tear-based gouty arthritis diagnosis using surface-enhanced raman scattering, ACS Nano 11 (2017) 438–443.
[23] T.T. Zheng, Z.G. Gao, Y. Luo, X.M. Liu, W.J. Zhao, B.C. Lin, Manual-slide-engaged paper chip for parallel SERS-immunoassay measurement of clenbuterol from swine hair, Electrophoresis 37 (2016) 418–424.
[24] Q. Liu, J.H. Wang, B.K. Wang, Z. Li, H. Huang, C.Z. Li, X.F. Yu, P.K. Chu, Paper-based plasmonic platform for sensitive, noninvasive, and rapid cancer screening, Biosens. Bioelectron. 54 (2014) 128–134.
[25] H. Torul, H. Ciftci, D. Cetin, Z. Suludere, I.H. Boyaci, U. Tamer, Paper membrane-based SERS platform for the determination of glucose in blood samples, Anal. Bioanal. Chem. 407 (2015) 8243–8251.
[26] C. Shen, J. Wang, Y. Cao, Y. Lu, Facile access to B-doped solid-state fluorescent carbon dots toward light emitting devices and cell imaging agents, J. Mater. Chem. C 3 (2015) 6668–6675.
[27] S.W. Hu, S. Qiao, B.Y. Xu, X. Peng, J.J. Xu, H.Y. Chen, Dual-functional carbon dots pattern on paper chips for Fe^{3+} and ferritin analysis in whole blood, Anal. Chem. 89 (2017) 2131–2137.
[28] Y. Zhao, X. Pan, L. Zhang, Y. Xu, C. Li, J. Wang, J. Ou, X. Xiu, B. Man, C. Yang, Dense AuNP/MoS2 hybrid fabrication on fiber membranes for molecule separation and SERS detection, RSC Adv. 7 (2017) 36516–36524.
[29] M. Li, Y.H. Wang, Y. Zhang, J.H. Yu, S.G. Ge, M. Yan, Graphene functionalized porous Au-paper based electrochemiluminescence device for detection of DNA using luminescent silver nanoparticles coated calcium carbonate/carboxymethyl chitosan hybrid microspheres as labels, Biosens. Bioelectron. 59 (2014) 307–313.
[30] J.R. Gonzalez-Moya, Y. Garcia-Basabe, M.L.M. Rocco, M.B. Pereira, J.L. Principal, L.C. Almeida, C.M. Araujo, D.G.F. David, A.F. da Silva, G. Machado, Effects of the large distribution of CdS quantum dot sizes on the charge transfer interactions into TiO2 nanotubes for photocatalytic hydrogen generation, Nanotechnology 27 (2016) 285401.
[31] X.B. Wei, C.L. Shao, X.H. Li, N. Lu, K.X. Wang, Z.Y. Zhang, Y.C. Liu, Facile in situ synthesis of plasmonic nanoparticles-decorated g-C3N4/TiO2 heterojunction nanofibers and comparison study of their photosynergistic effects for efficient photocatalytic H-2 evolution, Nanoscale 8 (2016) 11034–11043.
[32] J.D. Shao, L.P. Tong, S.Y. Tang, Z.N. Guo, H. Zhang, P.H. Li, H.Y. Wang, C. Du, X.F. Yu, PLLA nanofibrous paper-based plasmonic substrate with tailored hydrophilicity for focusing SERS detection, ACS Appl. Mater. Interfaces 7 (2015) 5391–5399.
[33] X.X. Yang, O. Forouzan, T.P. Brown, S.S. Shevkoplyas, Integrated separation of blood plasma from whole blood for microfluidic paper-based analytical devices, Lab Chip 12 (2012) 274–280.
[34] D.W. Kufe, Mucins in cancer: function, prognosis and therapy, Nat. Rev. Cancer 9 (2009) 874–885.
[35] X.Y. Jiang, H.J. Wang, H.J. Wang, R. Yuan, Y.Q. Chai, Signal-switchable electrochemiluminescence system coupled with target recycling amplification strategy for sensitive mercury ion and Mucin 1 assay, Anal. Chem. 88 (2016) 9243–9250.
[36] C.S.M. Ferreira, C.S. Matthews, S. Missailidis, DNA aptamers that bind to MUC1 tumour marker: design and characterization of MUC1-binding single-stranded DNA aptamers, Tumor Biol. 27 (2006) 289–301.
[37] J.J. Feng, X.L. Wu, W. Ma, H. Kuang, L.G. Xu, C.L. Xu, A SERS active bimetallic core-satellite nanostructure for the ultrasensitive detection of Mucin-1, Chem. Commun. 51 (2015) 14761–14763.
[38] Y. He, Y. Lin, H.W. Tang, D.W. Pang, A graphene oxide-based fluorescent aptasensor for the turn-on detection of epithelial tumor marker mucin 1, Nanoscale 4 (2012) 2054–2059.
[39] C. Novara, F. Petracca, A. Virga, P. Rivolo, S. Ferrero, A. Chiolerio, F. Geobaldo, S. Porro, F. Giorgis, SERS active silver nanoparticles synthesized by inkjet printing on mesoporous silicon, Nanoscale Res. Lett. 9 (2014) 527.